DOI: 10.1002/adfm.200600751

Versatile Supramolecular Nanovalves Reconfigured for Light Activation**

By *Thoi D. Nguyen*, *Ken C.-F. Leung*, *Monty Liong*, *Yi Liu*, *J. Fraser Stoddart*,* and *Jeffrey I. Zink**

All autonomous machines share the same requirement—namely, they need some form of energy to perform their operations and nanovalves are no exception. Supramolecular nanovalves constructed from [2]pseudorotaxanes—behaving as dissociatable complexes attached to mesoporous silica which acts as a supporting platform and reservoir—rely on donor-acceptor and hydrogen bonding interactions between the ring component and the linear component to control the ON and OFF states. The method of operation of these supramolecular nanovalves involves primarily the weakening of these interactions. The [2]pseudorotaxane [BHEEEN⊂CBPQT]$^{4+}$ [BHEEEN ≡ 1,5-bis[2-(2-(2-hydroxyethoxy)ethoxy)ethoxy]naphthalene and CBPQT^{4+} ≡ cyclobis(paraquat-*p*-phenylene)], when this 1:1 complex is tethered on the surface of the mesoporous silica, constitutes the supramolecular nanovalves. The mesoporous silica is charged against a concentration gradient with luminescence probe molecules, e.g., tris(2,2′-phenylpyridyl)iridium(III), Ir(ppy)$_3$ (ppy = 2,2′-phenylpyridyl), followed by addition of CBPQT·4Cl to form the tethered [2]pseudorotaxanes. This situation corresponds to the OFF state of the supramolecular nanovalves. Their ON state can be initiated by reducing the CBPQT^{4+} ring with $NaCNBH_3$, thus weakening the complexation and causing dissociation of the CBPQT^{4+} ring away from the BHEEEN stalks on the mesoporous silica particles MCM-41 to bring about ultimately the controlled release of the luminescence probe molecules from the mesoporous silica particles with an average diameter of 600 nm. This kind of functioning supramolecular system can be reconfigured further with built-in photosensitizers, such as tethered 9-anthracenecarboxylic acid and tethered [Ru(bpy)$_2$(bpy(CH$_2$OH)$_2$)]$^{2+}$ (bpy = 2,2′-bipyridine). Upon irradiation with laser light of an appropriate wavelength, the excited photosensitizers transfer electrons to the near-by CBPQT^{4+} rings, reducing them so that they dissociate away from the BHEEEN stalks on the surface of the mesoporous silica particles, leading subsequently to a controlled release of the luminescent probe molecules. This control can be expressed in both a regional and temporal manner by the use of light as the ON/OFF stimulus for the supramolecular nanovalves.

1. Introduction

Our ability to create and engineer nanovalves is progressing apace with an eye on applications in areas such as controlled delivery of drugs, microfluidic devices, and lab-on-a-chip sensors. Our previous work involves the fabrication of pseudorotaxane-derivatized supramolecular nanostructured thin films,[1] supramolecular[2,3] and molecular[4] nanovalves that can be activated by redox chemistry and by pH changes, and the powering of a supramolecular machine with a photoactive molecular triad.[5,6] Other examples,[7–15] using a variety of methods of operation and activation, have been described in the literature. Some are based on photo-driven systems involving cis–trans isomerization of N=N double bonds in, for example, azobenzene derivatives, tethered to the walls of nanoporous membranes: such a configurational change can function[7] as a regulatory mechanism for mass transport through the channels of nanoporous materials. Light has been used to induce the intermolecular dimerization of tethered coumarins in the knowledge that these dimers can act[8,9] as a kind of net to control access to and from the nanopores of derivatized silica particles MCM-41. Alternatively, redox chemistry has been used[10] to activate chemically-linked cadmium sulfide nanoparticles on derivatized mesoporous silica nanospheres where the nanoparticles function as caps to control the release of guests from the nanopores. In both these latter two examples, covalent bonds are made in order to trap guest molecules, and broken in order to release them, illustrating the inroads that dynamic covalent chemistry[11] is making into the operation of such devices. A heat-responsive polymer, poly(*N*-isopropylacrylam-

[*] Prof. J. F. Stoddart, Prof. J. I. Zink, Dr. T. D. Nguyen,[+] Dr. K. C.-F. Leung,[++] Dr. Y. Liu, M. Liong
California NanoSystems Institute and
Department of Chemistry and Biochemistry
University of California, Los Angeles
405 Hilgard Avenue, Los Angeles, CA 90095-1569 (USA)
E-mail: stoddart@chem.ucla.edu, zink@chem.ucla.edu

[+] Current address: Advanced Technology and Systems Analysis Division, Center for Naval Analyses, 4825 Mark Center Dr., Alexandria, VA 22311, USA.

[++] Current address: Center of Novel Functional Molecules, Department of Chemistry, The Chinese University of Hong Kong, Shatin, NT, Hong Kong SAR, P.R. China.

[**] We thank Professor Mark Thompson (University of Southern California) for providing us with a sample of Ir(ppy)$_3$. We acknowledge a discussion with Drs. Alberto Credi and Edward Plummer about possible pathways of light activation, Dr. Johnny Skelton for early help with experimental setup and, Dr. Sourav Saha for manuscript preparation. The powder XRD instrument used in this work was obtained under equipment grant number DMR-0315828. This research was supported by NSF grants DMR-0346601 and CHE-0507929.

© 2007 WILEY-VCH Verlag GmbH & Co. KGaA, Weinheim

ide) (PNIPAAm), has also been employed[12] as the source of restriction at the pores' orifices to modulate the transport of solutes, albeit in an irreversible way. By utilizing monolithic copolymers to define the nanopores with tunable sizes, ranging from 10 to 1000 nm in diameter, PNIPAAm has been shown[13] to behave as a reversible nanovalve in microfluidic chips. Although not a mechanical valve as such, an ingenious way for turning the channel protein into light-actuated molecular valves has been reported.[14] In this system, a channel-appended photosensitizer with a spiropyran core undergoes photochemical ring opening, resulting in a charged zwitterionic merocyanine structure. This formation of a charged compound triggers the opening of the channel protein by means of a hydrophilic/hydrophobic mechanism. Supramolecular systems have also been employed to control the operation of nanovalves. For example, because of the pH-sensitive intermolecular hydrogen bonds between poly(ethyloxazoline) and poly(methacrylic acid), polymer gels can be addressed electrically,[15] leading to the release of trapped insulin molecules.

For future applications, it is most desirable to develop nanovalves with multiple activation mechanisms, such that they are responsive to benign stimuli that are applicable to biological systems. The movable elements of bistable rotaxanes are attractive for deployment[16–24] in such versatile molecular nanovalves, on account of their highly predictable responsiveness to light, redox processes, and pH stimuli. Although a lot less easy to cycle, supramolecular nanovalves,[2] based on [2]pseudorotaxanes, are much simpler in their design, synthesis and fabrication. Opening of these nanovalves only requires decomplexation of the rings from the stalks attached to the mesoporous nanoparticles. Dissociation of cyclobis(paraquat-*p*-phenylene) ($CBPQT^{4+}$) tetracationic rings, for example, from 1,5-bis[2-(2-(2-hydroxyethoxy)ethoxy)ethoxy]naphthalene (BHEEEN) threads/stalks in [2]pseudorotaxanes can be induced[25] by reduction of the ring with reducing agents such as $NaCNBH_3$. The same dissociation process can be integrated with a photosensitizer, such that the photo-excited state of the photosensitizer acts[26,27] as a powerful reductant that causes dissociation of the $CBPQT^{4+}$ ring from the BHEEEN stalk in the [2]pseudorotaxane in the presence of light. In this paper, the construction and operation of versatile supramolecular nanovalves, that employ (Fig. 1) both a reducing agent and light as the operation stimuli, are described. Based on a previous design[2] of supramolecular nanovalves in which a $[BHEEEN \subset CBPQT]^{4+}$ pseudorotaxane was used as the basis for control by redox chemistry, herein we describe a second generation of supramolecular nanovalves, which have been constructed from a different type of mesoporous silica, MCM-41 silica bead. We also discuss how their method of activation has been modified to include light-activation employing built-in photosensitizers.

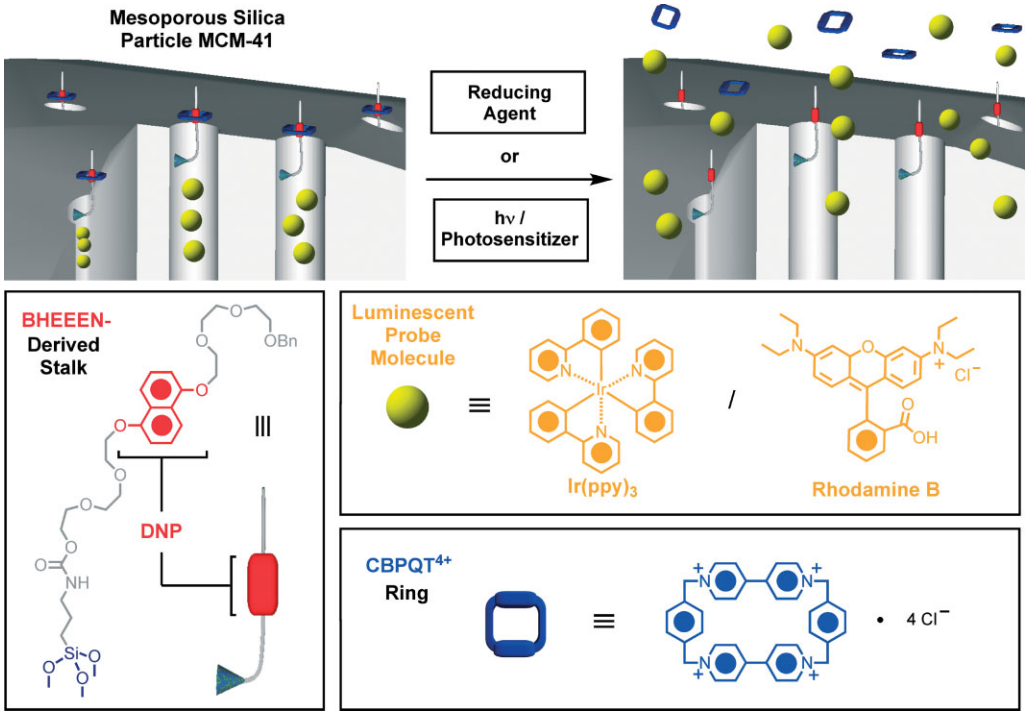

Figure 1. Schematic representations of the components of the supramolecular nanovalve, the assembled nanovalves, and the nanovalves' modes of activation. The BHEEEN stalk is attached to the mesoporous silica surface. After loading, the supramolecular nanovalves are capped (closed). The controlled release of luminescent probe molecules (opening of the nanovalves) from the supramolecular nanovalves is triggered by weakening the donor-acceptor interactions between the BHEEEN stalks and the $CBQPT^{4+}$ rings. The controlled release can be performed by a chemical reduction or photoactivation with built-in photosensitizers.

© 2007 WILEY-VCH Verlag GmbH & Co. KGaA, Weinheim

ADVANCED FUNCTIONAL MATERIALS

2. Results and Discussion

2.1. Preparation of Supramolecular Nanovalves

The nanoscale mesoporous particles, serving as both the solid support for the movable components and the containers for the probe molecules, were prepared[28–40] by surfactant-directed self-assembly to yield ordered arrays of tubes in sol-gel derived silica. The nanostructured silica, MCM-41, consists of near-spherical silica particles with an average diameter of 600 nm, as verified (Fig. 2A) by scanning electron microscopy (SEM). Using cetyltrimethylammonium bromide as the template, the ordered pores form a two-dimensional hexagonal structure that has a lattice spacing of 3.6 nm, as measured (Fig. 2B) by powder X-ray diffraction (XRD). The surfactant was removed by calcination for 5 h at 550 °C. N_2 Adsorption/desorption isotherms at 77 K were used (Fig. 2C) to determine the porosity of the material, which was shown to exhibit a high surface area (929.7 $m^2 g^{-1}$). By employing the Barret–Joyner–Halenda method of calculation, the inner diameters of the pores were estimated to be 2 nm.[31]

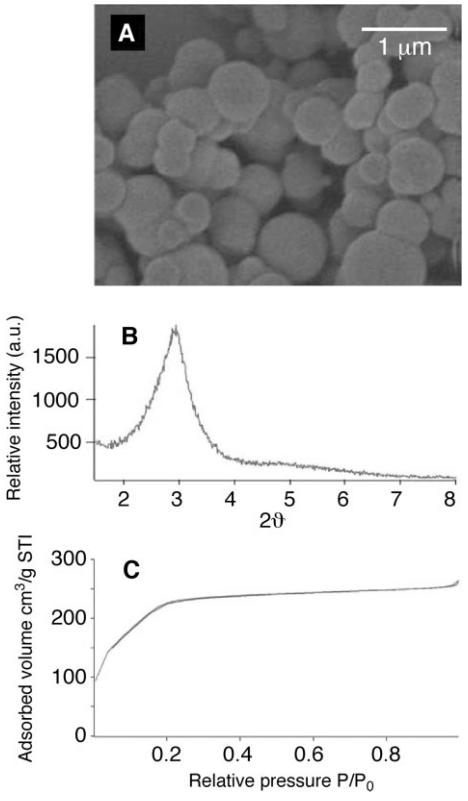

Figure 2. Measurement of the physical properties of mesoporous silica beads [38] by A) SEM, B) powder XRD, and C) N_2 adsorption/desorption isotherm. The mesoporous material consists of spherical silica particles with an average diameter of 600 nm, and has a lattice spacing of 3.6 nm.

The integration of the movable components with the nanostructured silica involves the derivatization of MCM-41 with isocyanatopropyltriethoxysilane (ICPES), which serves as the linker between arrays of pseudorotaxanes and the silica surface. The coupling between ICPES and the silica was carried out by a vapor-phase reaction[41] between the silanol groups on the surfaces of the nanostructured silica and the ICPES. The monobenzylated[1] BHEEEN was coupled with the isocyanate functions on ICPES, forming carbamate linkages. The successful attachment of BHEEEN to the MCM-41 surface was confirmed by monitoring (Fig. 3A) the emission spectrum of the dioxynaphthalene (DNP) unit of BHEEEN. Mer-Ir(ppy)$_3$ (ppy = 2,2′-phenylpyridyl) was chosen as a probe for controlled release, because it has intense luminescence that can be monitored (Fig. 3B) conveniently, while it is compatible with the reduction of $CBPQT^{4+}$ rings with $NaCNBH_3$ that triggers its controlled release. The loading of the probe molecules into the MCM-41 was confirmed by the luminescence spectrum (Fig. 3C) of the Ir(ppy)$_3$, trapped in the mesoporous silica particles. The difference between the emission spectra shown in Figure 3A and B (the probe molecule in solution and inside the pores, respectively) is caused by the effect of the surrounding medium on the luminescence spectrum (solvatochromism). Solvatochromism is large for molecules with metal to ligand charge transfer excited states as is the case here. The shift provides strong evidence that the probe is in a different environment (in the pore) but not in solution.

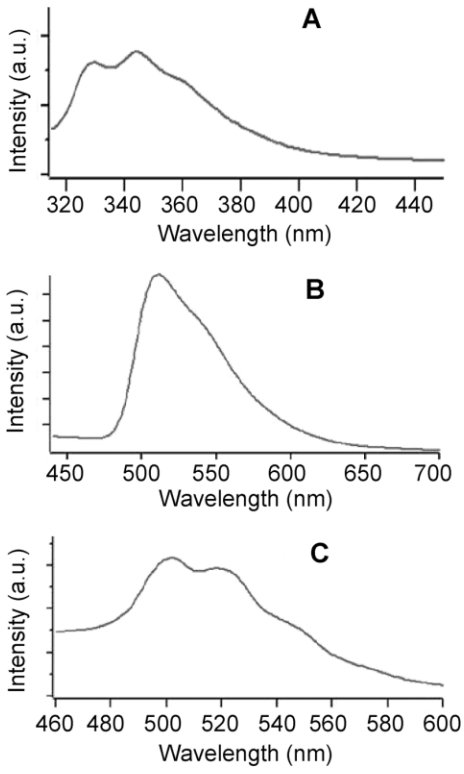

Figure 3. Luminescence spectra of the components of the supramolecular nanovalve. The spectra for A) the DNP moiety of the BHEEEN stalk on the MCM-41 material after derivatization, B) mer-Ir(ppy)$_3$, the probe molecule in solution, and C) the Ir(ppy)$_3$ probe molecule in MCM-41 material after loading are shown. Note the wavelength scales are different.

In order to cap the nanopores by closing the supramolecular nanovalves, the BHEEEN-derivatized silica material was

 © 2007 WILEY-VCH Verlag GmbH & Co. KGaA, Weinheim

soaked in an aqueous solution of CBPQT·4Cl. The complete system (trapped probe molecules with closed nanovalves) was then rinsed with PhMe to wash away any probe molecules that were sitting on the surface or were present in the open pores. Evidence for the capping of the nanopores with $CBPQT^{4+}$ rings was provided by the quenching of the DNP luminescence. The emission of the DNP subunits in the BHEEEN stalks on the silica was quenched by a factor of 2.3 after their complexation with $CBPQT^{4+}$ rings, an observation which is consistent with the quenching behavior observed[26,27] in solution previously.

2.2. Operation of the Supramolecular Nanovalves Triggered by Chemical Reduction

The operation of the nanovalves constructed from the $[BHEEEN \subset CBPQT]^{4+}$ pseudorotaxanes on MCM-41 is similar to that reported[2] previously for the nanovalves on silica thin films. The release of the probe molecules, $Ir(ppy)_3$, from the functional material into solution was monitored over time using luminescence spectroscopy. Additional evidence for the nanovalves' operation was obtained by following the DNP luminescence before and after the nanovalves' operation.

The controlled release of $Ir(ppy)_3$ from the nanopores into the solvent system (1:1, EtOH/PhMe), after the opening of the nanovalves with a reducing agent ($NaCNBH_3$), was monitored (Fig. 4) using luminescence spectroscopy. The functional material was placed (Scheme 1) at the bottom of a quartz cell, which was then filled carefully with the solvent system to ensure a clear solution. The cell was placed in the cell holder,

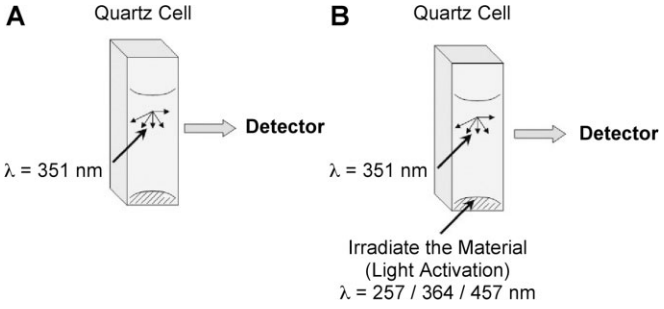

Scheme 1. Schematic diagram of the excitation geometry of the controlled release experiments. (A) Redox activation of the supramolecular nanovalves is monitored by the detection of probe molecules released into the solution by luminescence spectroscopy. (B) Light activation of the supramolecular nanovalves utilizes a second laser line to irradiate the materials.

such that only the liquid above the solid MCM-41 powder was exposed to the excitation light beam. This setup allows the observation of the $Ir(ppy)_3$ released into solution but not the trapped $Ir(ppy)_3$ in the nanopores. The solution was stirred extremely slowly to ensure mixing. Initially, there was little emission intensity of $Ir(ppy)_3$ in solution, attesting to minimal leakage by the supramolecular nanovalves (Fig. 4A). After about 100 s, 0.1 mL of $NaCNBH_3$ in a 1:1 EtOH/PhMe solution (80 mM) was added carefully. An increase in the luminescence

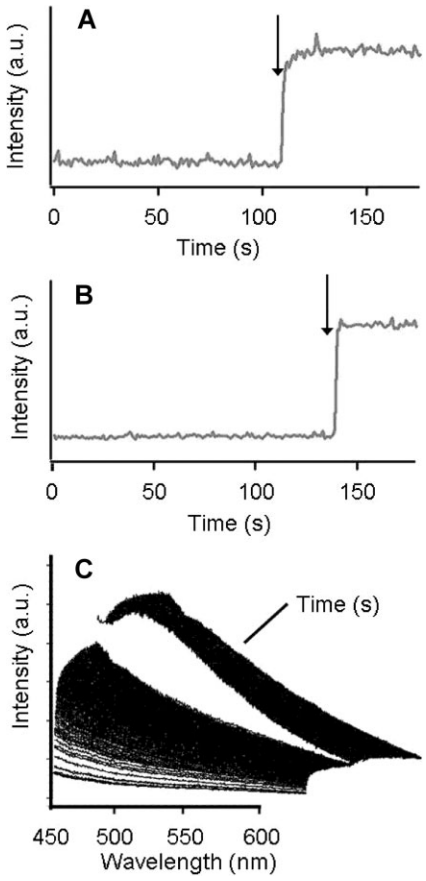

Figure 4. Controlled release profiles of $Ir(ppy)_3$ from supramolecular nanovalves using $NaCNBH_3$ as the reducing agent. A) The first cycle of controlled release, and B) the second cycle of controlled release after reloaded and recapped the supramolecular nanopores. C) The three-dimensional luminescence spectra of the probe molecules from the controlled release with time (excitation wavelength = 351 nm). The arrow indicates the activation time. For (A) and (B), the intensity axis are in the same scale.

intensity of $Ir(ppy)_3$ was observed (Fig. 4A) in response to the addition of the reducing agent which opens the supramolecular nanovalves, indicating that $Ir(ppy)_3$ was released from the nanopores into the solution. After the controlled release, the nanovalves were recycled by recharging the probe molecules into the nanopores and subsequent capping the BHEEEN stalks with $CBPQT^{4+}$ rings. The recycled nanovalves showed (Fig. 4B) controlled release, demonstrating the reversibility of the molecular recognition motif and the reusability of the functional material. The luminescence spectra of the probe molecules accumulating in solution were recorded with time (Fig. 4C) during the release process.

The operation of the supramolecular nanovalves can also be monitored directly from the luminescence of the DNP units on the BHEEEN stalks, since it increases (Fig. 5A and B) upon the addition of $NaCNBH_3$, indicating that the supramolecular nanovalves have been opened and the DNP luminescence is no longer quenched by the reduced $CBPQT^{4+}$ rings as a result. Control experiments were carried out to establish that the increase in $Ir(ppy)_3$ intensity upon the addition of $NaCNBH_3$

© 2007 WILEY-VCH Verlag GmbH & Co. KGaA, Weinheim

ADVANCED FUNCTIONAL MATERIALS

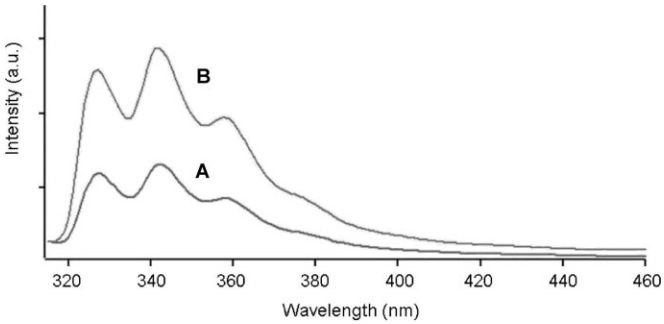

Figure 5. The supramolecular nanovalves' operations were monitored by the DNP luminescence. In its closed state, when the $CBPQT^{4+}$ ring encircles the DNP unit, DNP luminescence is quenched (A). When the supramolecular nanovalves are opened, the rings dissociate from the stalks and the DNP luminescence increases (B).

was not the result of some other factor. Addition of reducing agent to the supramolecular nanovalves that were not filled with probe molecules caused no emission, showing that the reducing agent is not producing a spurious luminescence. Functional materials derivatized with BHEEEN stalks and loaded with $Ir(ppy)_3$ did not retain the probe molecules after washing, as indicated by the fact that, when they are introduced into the cell, no change in emission is observed after the addition of the reducing agent. These control experiments confirm that the $CBPQT^{4+}$ rings are required in order to close the supramolecular nanovalves, thus trapping the probe molecules.

In order to verify that the change in emission caused by the addition of the reducing agent is a result of dissolved probe molecules released from the nanopores, but not a result of suspended MCM-41 particles, the particles were doped with uranyl ions, which act as a luminescent internal standard. The presence of the uranyl ions in the functional material can be verified by its characteristic emission spectra.[42] Using the uranyl ions' emission as an internal standard, the ratio of $Ir(ppy)_3$ concentration to the uranyl ions' concentration before opening of the supramolecular nanovalves is higher than that after opening, an observation which is consistent with the release of $Ir(ppy)_3$ from the porous silica material into solution. In addition, the ratio of DNP to uranyl ions' emission intensities increases after the opening of the nanovalves. A small emission from uranyl ions was observed during the controlled release, indicating that some of the suspended particles were present in the excitation beam. No change in its intensity was observed, however, during the operation of the nanovalves when the trapped probe molecules were released.

2.3. Preparation of Supramolecular Nanovalves with Built-in Photosensitizers

The expansion of the mechanism of operation of nanovalves to include photoactivation represents a significant step towards the use of less harsh and gentler forms of energy for opening supramolecular nanovalves. The use of light energy also increases considerably the pool of probe molecules: operating the nanovalves using $NaCNBH_3$ limits severely the probe molecules that can be studied because of cross reactivity with the reductant. There are several ways to adapt a system that works by chemical (redox) activation to one that is operated by light. One way is to carry out the photolytic reduction of the $CBPQT^{4+}$ rings by using a photosensitizer dissolved in the same solution as the rings. For example, the $[BHEEEN \subset CBPQT]^{4+}$ pseudorotaxane can be dissociated[26,27] using 9-anthracenecarboxylic acid (ACA) as the photosensitizer ($E^\circ = -0.88$ V versus SCE, lifetime = 250 μs). $Ru^{II}(bpy)_3$ ($E^\circ = -0.80$ V versus SCE, lifetime = 13 μs) has also been added to the solution in order to photosensitize the dissociation of the [2]pseudorotaxane stalks, albeit with less efficiency because of the much shorter lifetime of this complex in its excited state.[26,27,43] Alternatively, photosensitizers can be connected[44] covalently to the stalk so that they can transfer electrons efficiently to the $CBPQT^{4+}$ ring. In the context of the construction of the supramolecular nanovalves, the photoinduced electron transfer can be facilitated[45–47] by positioning the photosensitizers on the nanoporous material's surface in close proximity to the nanovalves. In this case, the entire particle-nanovalves-built-in power supply is one integrated unit.

Tethering of the photosensitizers to the surface of the mesoporous silica in the proximity of the nanovalves gives (Fig. 6) a functional material with built-in transducers. After the tethering of BHEEEN to the silica surface, the photosensitizers were then tethered[48] to the functional material. The tethered BHEEEN prevents the photosensitizers from diffusing into the nanopores, thus constraining them to the outer surface of the nanopores.[49] The photosensitizers were attached using a much larger concentration than that of the stalks, resulting in a high coverage ratio of photosensitizers to nanovalves. The successful incorporation of ACA onto the MCM-41 was confirmed by monitoring the luminescence signature of ACA from extensively-washed samples.

2.4. Operation of Supramolecular Nanovalves with Built-in Photosensitizers

The monitoring of supramolecular nanovalves with built-in photosensitizers triggered by light is similar to that initiated by chemical reduction. Instead of adding reducing agents, light with appropriate wavelengths—364 nm for ACA and 457 nm for $Ru^{II}(bpy)_3$—is used (Scheme 1) to irradiate the material at the bottom of the cuvette. The selection of the laser line depends on the absorption maximum of the photosensitizers. In these experiments, the 351 nm laser line was kept continuously switched ON to excite the released probe molecules for detection. A sacrificial reducing agent—triethanolamine—was added to regenerate the neutral sensitizer and inhibit the reverse process, namely oxidation of the reduced $CBPQT^{4+}$ ring from taking place.

The release of $Ir(ppy)_3$ from the nanopores upon light activation was monitored (Fig. 7) by luminescence spectroscopy. For the nanovalves with built-in ACA, the system was left unactivated in solution to establish a baseline and to demonstrate no leakage. Upon irradiation of the nanoporous material with 364 nm laser excitation, a slow increase in the luminescence in-

 © 2007 WILEY-VCH Verlag GmbH & Co. KGaA, Weinheim

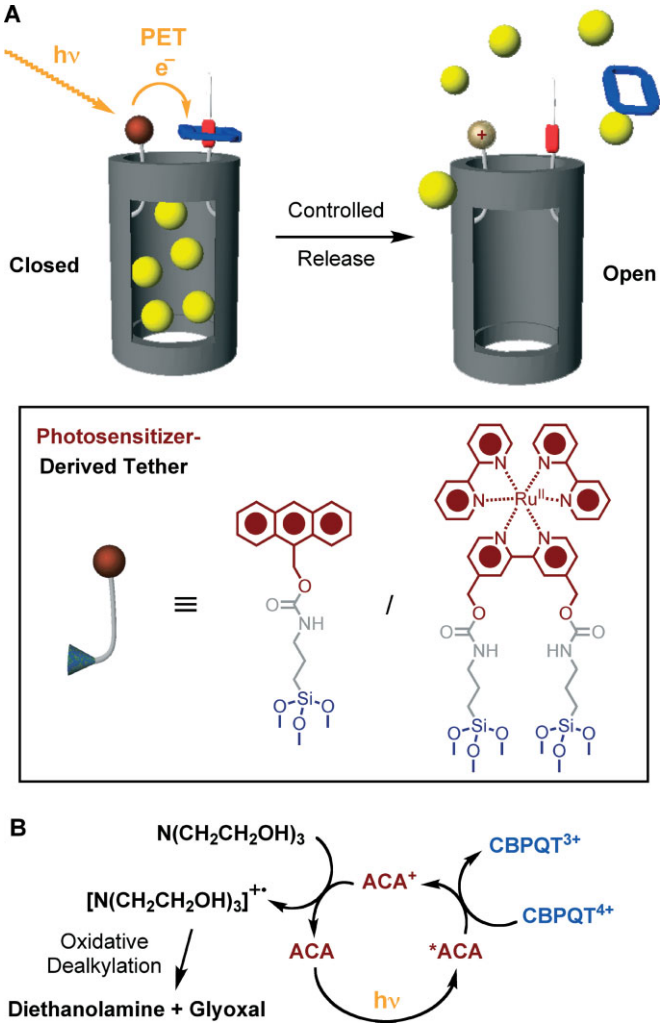

Figure 6. A) 9-Anthracenecarboxylic acid (ACA) and $Ru^{II}(bpy)_2(bpy(-CH_2OH)_2)$ as photosensitizers attached to the nanopores on the mesoporous silica in the photoexcited electron transfer (PET) cycle. B) The cycle depicts the role of triethanolamine as sacrificial reducing agent, which reduces the ACA^+ moiety into ACA again and then undergoes an oxidative dealkylation to give diethanolamine and glyoxal.

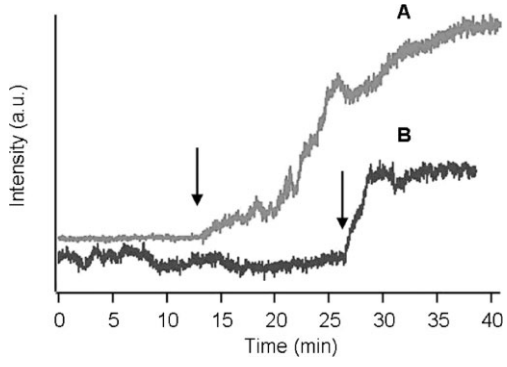

Figure 7. Controlled release profiles of $Ir(ppy)_3$ by photoactivation from the supramolecular nanovalves having A) ACA and B) $Ru^{II}(bpy)_3$ as sensitizer. The arrow indicates the time at which light is turned on to excite the material. For (A), a 351 nm laser line was used. For (B), a 457 nm laser line was used.

tensity was observed, caused by the release of $Ir(ppy)_3$ into the solution. For the nanovalves with built-in $Ru^{II}(bpy)_3$ photosensitizers, irradiation of the material with 488 nm laser light triggered the release of $Ir(ppy)_3$. The release rate of the $Ir(ppy)_3$ probe molecules by the $Ru^{II}(bpy)_3$-sensitized supramolecular nanovalves was faster than that from the ACA-sensitized nanovalves.

In order to correlate the triggered release process with the activation of the nanovalves, the luminescence of DNP was monitored before and after light activation. After photoactivation, the DNP emission of the material showed a 2.3-fold increase in intensity, similar to that shown in Figure 5. This result demonstrates that, in the supramolecular nanovalves with the built-in photo-transducer, light with the appropriate wavelength triggers the controlled release of $Ir(ppy)_3$ by causing the dissociation of the $CBPQT^{4+}$ rings as a result of photoexcited electron transfer from the sensitizers to the rings.

Since the change in the activation process from chemical reduction to light allows other luminescent probe molecules to be used, rhodamine B was selected on account of its similar size to $Ir(ppy)_3$. Irradiation of the supramolecular nanovalves with built-in ACA at 364 nm caused them to open, releasing (Fig. 8) rhodamine B into solution, as indicated by the increase in luminescence intensity. In contrast with the release of $Ir(ppy)_3$ where the release rate follows a sigmoid curve, the release of rhodamine B exhibits a much more constant rate of release.

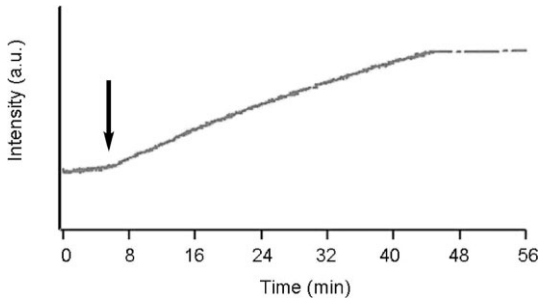

Figure 8. Photoactivated release profile of rhodamine B from the supramolecular nanovalves having built-in ACA. The arrow indicates the time light is turned on to excite the material. After 46 min, luminescence spectra of rhodamine B in solution were taken and their maximum intensities were plotted.

The total release times for both probe molecules using the nanovalves with built-in ACA are similar, suggesting that the rate of electron transfer from the photoexcited ACA to the $CBPQT^{4+}$ ring may be the rate-controlling process.

Comparison of the controlled release of rhodamine B and $Ir(ppy)_3$ from the supramolecular nanovalves indicates that the system activated by chemical reduction experiences a much faster rate of release than that activated by light employing built-in photosensitizers. This difference is accounted for, in part, by the experimental setup and in part, by the rate of photoexcited electron transfer. In the system that is chemically activated, the added $NaCNBH_3$ reduces the $CBPQT^{4+}$ rings rapidly. The rate of electron transfer from the excited state

© 2007 WILEY-VCH Verlag GmbH & Co. KGaA, Weinheim

ADVANCED FUNCTIONAL MATERIALS

photosensitizers to the $CBPQT^{4+}$ rings is influenced by the relative positioning of the photosensitizers and the $CBPQT^{4+}$ rings as well as by the availability of photons.[26,27] These controlled release rates correlate very well with the rate of dissociation of the $CBPQT^{4+}$ rings into solution triggered by reducing agents[25] and light.[26,27] Using a reducing agent as the stimulus, the dissociation of the $CBPQT^{4+}$ rings is fast, happened within a second, whereas when using light in the presence of photosensitizers, the dissociation rate is much slower, i.e., of the order of tens of minutes. Based on these correlations, the dissociation by whatever mechanism is the rate-controlling step.

However, the exact number of nanovalves available for actuation upon the stimuli is not clear because the number of nanovalves that are activated depends on the irradiation geometry and the light intensity among other factors. Under the experimental condition, about 10 % of the nanovalves are activated by light. After activating the nanovalves with light, all the nanovalves are activated with excess of $NaCNBH_3$ reducing agent and the ratio of the amount released by light activation to the total released by light and by the reducing agent was measured.

2.5. Control Experiments

In order to establish the relative importance of the components required for the functioning of the light-operated supramolecular nanovalves, a set of control experiments were carried out. Specifically, these experiments were designed to investigate the role of the sacrificial reducing agent and the built-in photosensitizers on the operation of the nanovalves. In two control experiments, (i) the light-activated supramolecular nanovalves were operated without any sacrificial reductant in order to determine the importance of the sacrificial reductant, and (ii) the supramolecular nanovalves without built-in photosensitizers were subjected to the same kind of irradiation to ascertain the role of the photosensitizers.

The sacrificial reducing agent plays an important role (Fig. 6B) in the operation of the nanovalves. In solution, the presence of a sacrificial reducing agent (triethanolamine) inhibits[26,27] the reverse oxidation process and enables the much slower nuclear movement (dissociation) of the $CBPQT^{3+}$ rings to take place. In order to determine if it is important for the efficient operation of the nanovalves, those materials with built-in ACA were studied without triethanolamine being present. Irradiation under conditions identical to those used in Section 4 showed (Fig. 9) that only a small amount of probe molecules was released. The rate of release is much slower than when the sacrificial electron donor is present (Fig. 7) and confirms the critical contribution that it plays in preventing the reverse oxidation process from $CBPQT^{3+}$ back to $CBPQT^{4+}$ and in regenerating ACA for continuing operation of the nanovalves.

The slow release (Fig. 9) of probe molecules in the absence of triethanolamine could result from thermal effects. At high temperatures, a small percentage of the $CBPQT^{4+}$ rings will dissociate from the pseudorotaxane. Thus, local heating, caused by irradiation could lead[50] to dissociation. In order to assess

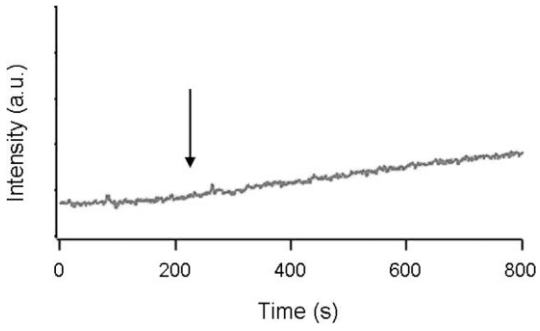

Figure 9. Controlled release profile of the supramolecular nanovalves with built-in ACA and rhodamine B as the probe molecules but without a sacrificial reducing agent, triethanolamine, in solution. The arrow indicates the time 351 nm laser light is turned ON.

the importance of local heating, light with a longer wavelength that is not absorbed by the photosensitizer was used to irradiate the nanovalves with built-in ACA. Irradiation of 457 nm with the same power as that used previously did not cause any observable release of the luminescent probe molecules. The slow release observed in the absence of triethanolamine is probably a result of the inefficient reduction of the $CBPQT^{4+}$ rings and not a result of local heating effects. These observations also rule out the possibility of dissociation being caused by direct excitation of the charge transfer band arising from the pseudorotaxane itself. According to this mechanism, irradiation transfers charge from excited DNP units to their encircling $CBPQT^{4+}$ rings, reducing them and causing them to dissociate.[51] Dissociation by this mechanism is therefore dependent on the excitation wavelength. Since 457 nm light excites the charge transfer band and no controlled release is observed, it is reasonable to rule out this pathway. The charge transfer excited state is extremely short lived and most likely will not allow the very much slower nuclear motion of the $CBPQT^{4+}$ ring to occur.

In order to verify the necessity of photosensitizers in the controlled-release process, the nanovalves without built-in photosensitizers were subjected to the same irradiation conditions. Surprisingly, after 364 nm irradiation, a very small increase of $Ir(ppy)_3$ in solution was observed. After 40 min of irradiation, a significant increase in emission intensity occurs and the DNP emission also increases. After 257 nm irradiation, a larger increase was observed (Table 1). The total release was much smaller than that observed with the photosensitized material, emphasizing the importance of the photosensitizers in trigger-

Table 1. Change in the luminescence of the supernatant solution after the supramolecular nanovalves, without photosensitizer and with $Ir(ppy)_3$ as the probe molecule, were exposed to light with different wavelengths.

	Excitation wavelength		
	257 nm	351 nm	488 nm
Intensity of laser	15 mW	15 mW	15 mW
Difference of $Ir(ppy)_3$ luminescence intensity (a.u.)	15000	5300	0

© 2007 WILEY-VCH Verlag GmbH & Co. KGaA, Weinheim

ing the dissociation. However, a less efficient mechanism, one that is responsible for this slow release, must be operating.

Two possible mechanisms with literature precedence[52–55] could explain the increase in $Ir(ppy)_3$ luminescence intensity in solution when the supramolecular nanovalves without photosensitizers were irradiated. The first mechanism is a modification of a pathway proposed[52–54] for the photochemistry of pseudorotaxanes entrapped in zeolite in which the zeolite acts (Fig. 10A) as an electron donor. Modifying this mechanism for the present silica-based nanovalves, it could be proposed that excitation excites $CBPQT^{4+}$ and then excited rings accept electrons from the silicon framework. The reduced rings could then dissociate and open the supramolecular nanovalves. The observed wavelength dependence supports this mechanism since 257 nm light triggered some release, 361 nm light triggered minimal release, but 457 nm light did not trigger any release at all. In a second possible mechanism, $Ir(ppy)_3$ could be acting (Fig. 10B) as both the probe molecule and the photosensitizer. According to this hypothesis, irradiation with UV light excites $Ir(ppy)_3$. In its excited state, $Ir(ppy)_3$* is a powerful reductant[55] ($E^\circ = -1.8$ V), capable of transferring an electron to the $CBPQT^{4+}$ rings. The reduction of the ring leads to dissociation and release of $Ir(ppy)_3$ from the nanopores. This mechanism should also be wavelength dependent as is observed—UV light induces a small release but visible light does not.

The use of rhodamine B as the probe molecule helps to differentiate between the two mechanisms because it is not a reductant in its excited state.[56] The release profile showed no release of rhodamine B molecules upon excitation at 257 nm, in contrast with the observed release of $Ir(ppy)_3$ from the supramolecular nanovalves without photosensitizers. This experiment suggests that the mechanism involving electron transport from silicon to the $CBPQT^{4+}$ rings is not operative and supports the hypothesis that the $Ir(ppy)_3$ is capable of acting as a photosensitizer. In the presence of ACA as the photosensitizers, release of both rhodamine B and $Ir(ppy)_3$ occur with high efficiencies.

2.6. Regional and Temporal Control

The ability to use light to operate supramolecular nanovalves and to control the release of probe molecules opens up new possibilities for a more sophisticated level of nanovalve control. Since light can be focused onto a small area, regional control of a sample can be effected. As a demonstration of this concept, a spot of about 200 μm was focused on the nanovalves. After irradiation had opened the nanovalves and released the probe molecules, a different region of the sample was irradiated and a further release occurred (Fig. 11A). Spatial control on the micron length scale is extremely difficult to achieve using chemical reductants.

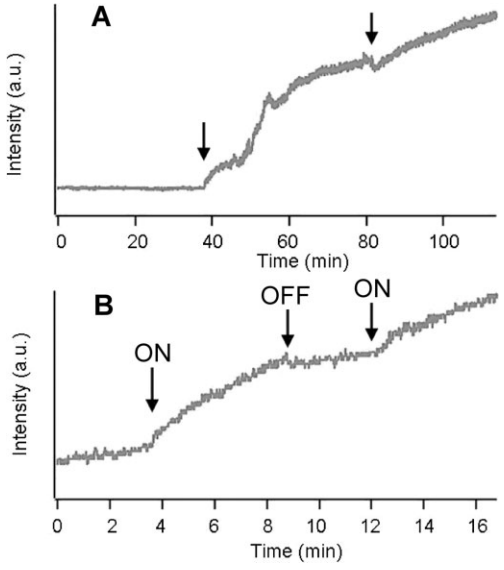

Figure 11. Regional and temporal controls of the supramolecular nanovalves with a built-in photosensitizer using light. A) After the entire content from one spot has been released, the light was focused on another spot as indicated by the arrow and B) the light focused on one spot but being turn ON and OFF and ON again at different time.

Light activation also allows temporal control of supramolecular nanovalves. In the irradiated region, the nanovalves open continuously at a rate determined by the intensity of the light but will not open when irradiation is stopped. Thus, the release of the trapped probe molecules can be started, stopped, and adjusted simply by controlling the light. A simple demonstration is illustrated in Figure 11B. When the light is turned ON, release commences, and when the light is turned OFF, it ceases. Release resumes when the light is turned ON again. While this type of control is theoretically possible by careful metering of chemical reagents, it is much easier using changes in light intensity.

When these systems involving the controlled release of rhodamine B and $Ir(ppy)_3$ are activated by chemical reagents, they exhibit a much faster rate of release than when they are activated by light and have built-in photosensitizers. This difference can be explained in part by the controlled release setup and in part

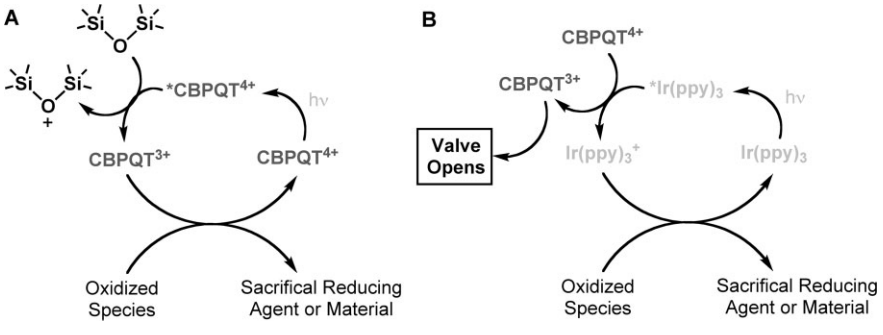

Figure 10. Possible mechanism for the background release from the material without photosensitizer upon light activation: A) the material acting as an electron donor and B) the probe molecule acting as a photosensitizer.

© 2007 WILEY-VCH Verlag GmbH & Co. KGaA, Weinheim

ADVANCED FUNCTIONAL MATERIALS

by the rate of photoexcited electron transfer. In the system that is chemically activated, the addition of $NaCNBH_3$ is presumed to reduce the $CBPQT^{4+}$ rings rapidly. In the system that is light activated,[26,27] the rate of electron transfer from ACA to the $CBPQT^{4+}$ rings is hindered by the relative positions of the ACA photosensitizer and the $CBPQT^{4+}$ rings as well as by the availability of photons. These controlled release rates correlate very well with the rates of dissociation in solution[25–27] triggered by reducing agents and by light. Using the reducing agent as the stimulus, the dissociation of the $CBPQT^{4+}$ rings from the [2]pseudorotaxane is fast and occurs on the order of seconds, whereas, when using light, even in the presence of photosensitizers, the rate of dissociation is very much slower, occurring on the order of tens of minutes. It follows that the rate of dissociation, by whatever mechanism, is the rate-determining step.

3. Summary

Supramolecular nanovalves, with multiple modes of activation, and constructed from donor-acceptor [2]pseudorotaxanes which act as gatekeepers, and mesoporous silica which acts as both a supporting platform for the gatekeepers and a reservoir for the probe molecules, have been demonstrated to work in more ways than one. In one mode of operation, a chemical reducing agent opens the gates. In another mode of operation, built-in photosensitizers have been used to attain this same objective, albeit light is much slower than the chemical reducing agent at activating the opening of the gates. Although reversibility is attainable and two cycles have been completed successfully, donor-acceptor supramolecular nanovalves lack the simplicity of operation that is attainable in this regard by their molecular counterparts. The relative ease of construction of supramolecular nanovalves, along with their potential to become highly modular in their construction, however, renders them attractive gatekeepers. Moreover, the fact that they can be designed to harness light for opening the gates leaves them wide open to regional and temporal control: both are features which enhance the potential applicability of supramolecular nanovalves.

4. Experimental

Materials: 1,5-Bis[2-(2-(2-hydroxyethoxy)ethoxy)ethoxy]naphthalene (BHEEEN) [57], cyclobis(paraquat-*p*-phenylene) ($CBPQT^{4+}$) tetrachloride [58] and $[Ru(bpy)_2(bpy(CH_2OH)_2)](2PF_6)$ [59] were synthesized according to literature procedures. Distilled and deionized H_2O were obtained from Millipore. Other analytical and reagent grade chemicals were purchased from the following suppliers and used without further purification—9-anthracenecarboxylic acid (ACA, 99%, Aldrich), tetraethoxysilane (TEOS, 98%, Aldrich), cetyltrimethylammonium bromide (CTAB, ≥99%, Aldrich), isocyanatopropyltriethoxysilane (95%, Aldrich, redistilled prior to use), PhMe (≥99.5%, EMD), NH_4OH solution (28–30%, EMD), EtOH (200 proof, Pharmaco-AAPER), rhodamine B (Lambda Physik), $Ir(ppy)_3$ (ppy = 2,2′-phenylpyridyl).

Instrumentation: Powder X-ray diffraction (XRD) patterns were collected using a Philips X'Pert Pro diffractometer equipped with Cu Kα radiation. Scanning electron microscopic (SEM) images were collected using a JEOL SM-71010 (fine powder profile) instrument. Au coating of the material for SEM imaging was carried out with a gold sputterer (Hummer 6.2, Anatech LTD, plasma discharge current = 15 mA at 70 mTorr for 2 min). N_2 isotherms were measured using a Micromeritics ASAP 2000 (mesoporous material program) instrument. The controlled release of probe molecules into solution was monitored over time by luminescence spectroscopy (Acton SpectraPro 2300i CCD, and Krypton Innova I300C and Argon Innova 90C-5 excitation lasers, and Fluorolog FL3-22 (ISA Spex, Jobin Yvon, Longjumeau, France)).

General Preparation of the Pseudorotaxane-MCM-41: MCM-41 was prepared according to literature procedures [28–30]. The doping of uranyl nitrate into the MCM-41 framework was carried out during the MCM-41 synthesis. Uranyl nitrate (0.63 g) was added to the surfactant solution prior to the addition of TEOS. Surfactants were removed by calcination at 550 °C for 5 h. Successful surfactant removal was confirmed by shifts in the Bragg peaks and also by the large increase in the volume of N_2 being adsorbed as indicated by N_2 isotherm. Attachment or incorporation of the functioning molecular components into the sol-gel materials have been achieved in the following manner [31–37]. The calcined MCM-41 was derivatized with isocyanatopropyltriethoxysilane (ICPES) using a gas-phase reaction: the powder was placed on a filter above the solution with the precursor of the linker in PhMe and heated under reflux for 12 h under N_2 (1 atm) [1,41]. The linker-derivatized material (ICPES-MCM-41) was soaked in PhMe for 1 d to remove the surface-adsorbed reagent, followed by filtering and drying under reduced pressure. Subsequently, the resulting linker-derivatized MCM-41 (1.70 g) was heated under reflux with a solution of BHEEEN (0.004 mmol, 0.5 mM) in the presence of N_2 (1 atm) to afford BHEEEN-MCM-41. The extensively washed material was tested for the presence of BHEEEN, based on the dioxynaphthalene (DNP) luminescence of the powdered material. The loading of the derivatized MCM-41 with guest (luminescent probe) molecules was achieved by soaking this porous material in a solution containing the guests (0.4–0.5 mM guest in 1:1 EtOH/PhMe). The loaded material was capped with $CBPQT^{4+}$ by soaking the material in an aqueous solution of CBPQT·4Cl (0.003 mmol, 0.3 mM). The loaded and closed supramolecular nanovalves were washed with 1:1 EtOH/PhMe to remove the surface-adsorbed guest molecules.

Integration of Photosensitizers into the Nanovalve: Photosensitizers were integrated into the supramolecular nanovalves after the preparation of BHEEEN-MCM-41. For the ACA derivatized nanovalves, BHEEEN-MCM-41 (260 mg) was heated under reflux in an EtOH solution of ACA (0.45 mmol, 18 mM, 25 mL) for 2 d. The solid material was filtered and soaked in EtOH for 2 d to remove the surface-absorbed ACA. The material was then filtered and dried under reduced pressure. For the $[Ru(bpy)_2(bpy(CH_2OH)_2)](PF_6)_2$-derivatized supramolecular nanovalves, BHEEEN-MCM-41 (260 mg) was heated under reflux in a MeCN solution of $[Ru(bpy)_2(bpy(CH_2OH)_2)](PF_6)_2$ (0.038 mmol, 1.5 mM, 25 mL) for 1 d. The material was filtered and soaked in MeCN for 1 d to remove excess of the Ru complex. The material was then filtered and dried under reduced pressure. For loading and capping the BHEEEN stalks, the procedures were similar to the synthetic steps described in the previous section.

Experimental Setup for Controlled Release: The release of probe molecules from the hybrid MCM-41 into the supernatant was measured by monitoring the emission spectrum in the solution above the MCM-41 powder (release profile). The material was piled up on the bottom in a large quartz cuvette. The solvent system (1:1 EtOH/PhMe) was slowly added to prevent disturbing the powder. Triethanolamine (99 μL, a sacrificial reducing agent) was added to the solution. One laser line (351 nm, 20 mW) was focused at the supernatant 90° to the detector and was employed to irradiate continuously the supernatant to excite the probe molecules being released and monitored by either photo-muliplier-tube/charge-coupled device (CCD). This CCD detector collects sequentially the luminescence spectra once per second, giving a three-dimensional plot of luminescence intensity, wavelength, and time, while confirming the identity of the molecules being released. The photo-muliplier-tube detector collects sequentially the maxium intensity at a particular wavelength of the probe molecules released into

 © 2007 WILEY-VCH Verlag GmbH & Co. KGaA, Weinheim

the solution. For the supramolecular nanovalves' operation triggered by the reductant, $NaCNBH_3$ solution (0.1 mL, 1:1 EtOH/PhMe, 80 mM) was added at a designated time. For light activation, a second laser line 90° to the detector with the appropriate wavelength (257, 364, or 457 nm, 12 mW) was focused on the sample pile at a designated time to trigger the controlled release. The solution was stirred very slowly (1.5 setting in Corning Stirrer/Hot plate) to help create a homogenous solution.

Received: August 17, 2006
Revised: January 4, 2007
Published online: August 2, 2007

[1] S. Chia, J. Cao, J. F. Stoddart, J. I. Zink, *Angew. Chem. Int. Ed.* **2001**, *40*, 2447.
[2] R. Hernandez, H.-R. Tseng, J. W. Wong, J. F. Stoddart, J. I. Zink, *J. Am. Chem. Soc.* **2004**, *126*, 3370.
[3] a) T. D. Nguyen, K. C.-F. Leung, M. Liong, C. D. Pentecost, J. F. Stoddart, J. I. Zink, *Org. Lett.* **2006**, *8*, 3363. b) K. C.-F. Leung, T. D. Nguyen, J. F. Stoddart, J. I. Zink, *Chem. Mater.* **2006**, *18*, 5919.
[4] a) T. D. Nguyen, H.-R. Tseng, P. C. Celestre, A. H. Flood, Y. Liu, J. F. Stoddart, J. I. Zink, *Proc. Natl. Acad. Sci. USA* **2005**, *102*, 10029. b) T. D. Nguyen, Y. Liu, S. Saha, K. C.-F. Leung, J. F. Stoddart, J. I. Zink, *J. Am. Chem. Soc.* **2007**, *129*, 626.
[5] a) S. Saha, L. E. Johansson, A. H. Flood, H.-R. Tseng, J. I. Zink, J. F. Stoddart, *Small* **2005**, *1*, 87. b) S. Saha, L. E. Johansson, A. H. Flood, H.-R. Tseng, J. I. Zink, J. F. Stoddart, *Chem. Eur. J.* **2005**, *11*, 6846.
[6] S. Saha, K. C.-F. Leung, T. D. Nguyen, J. F. Stoddart, J. I. Zink, *Adv. Funct. Mater* **2007**, *17*, 685.
[7] N. Liu, D. R. Dunphy, P. Atanassov, S. D. Bunge, Z. Chen, G. P. López, T. J. Boyle, C. J. Brinker, *Nano Lett.* **2004**, *4*, 551.
[8] N. K. Mal, M. Fujiwara, Y. Tanaka, *Nature* **2003**, *421*, 350.
[9] N. K. Mal, M. Fujiwara, Y. Tanaka, T. Taguchi, M. Matsukata, *Chem. Mater.* **2003**, *15*, 3385.
[10] C.-Y. Lai, B. G. Trewyn, D. M. Jeftinija, S. Xu, S. Jeftinija, V. S.-Y. Lin, *J. Am. Chem. Soc.* **2003**, *125*, 4451.
[11] S. J. Rowan, S. J. Cantrill, G. R. L. Cousins, J. K. M. Sanders, J. F. Stoddart, *Angew. Chem. Int. Ed.* **2002**, *41*, 898.
[12] Q. Fu, G. V. Rama Rao, L. K. Ista, Y. Wu, B. P. Andrzejewski, L. A. Sklar, T. L. Ward, G. P. Lopez, *Adv. Mater.* **2003**, *15*, 1262.
[13] Q. Luo, S. Mutlu, Y. B. Gianchandani, F. Svec, J. M. J. Fréchet, *Electrophoresis* **2003**, *24*, 3694.
[14] A. Kocer, M. Walko, W. Meijberg, B. L. Feringa, *Science* **2005**, *309*, 755.
[15] I. C. Kwon, Y. H. Bae, S. W. Kim, *Nature* **1991**, *354*, 291.
[16] V. Balzani, A. Credi, F. M. Raymo, J. F. Stoddart, *Angew. Chem. Int. Ed.* **2000**, *39*, 3348.
[17] V. Balzani, A. Credi, M. Venturi, in *Molecular Devices and Machines—A Journey into the Nano World*, Wiley-VCH, Weinheim **2003**.
[18] Y. Liu, A. H. Flood, P. A. Bonvallet, S. A. Vignon, B. N. Northrop, H.-R. Tseng, J. O. Jeppesen, T. J. Huang, B. Brough, M. Baller, S. Magonov, S. Solares, W. A. Goddard, III, C.-M. Ho, J. F. Stoddart, *J. Am. Chem. Soc.* **2005**, *127*, 9745.
[19] V. Balzani, A. Credi, B. Ferrer, S. Silvi, M. Venturi, *Top. Curr. Chem.* **2005**, *262*, 1.
[20] F. Aricó, J. D. Badjić, S. J. Cantrill, A. H. Flood, K. C.-F. Leung, Y. Liu, J. F. Stoddart, *Top. Curr. Chem.* **2005**, *249*, 203.
[21] N. N. P. Moonen, A. H. Flood, J. M. Fernández, J. F. Stoddart, *Top. Curr. Chem.* **2005**, *262*, 99.
[22] E. R. Kay, D. A. Leigh, *Top. Curr. Chem.* **2005**, *262*, 133.
[23] A. B. Braunschweig, B. H. Northrop, J. F. Stoddart, *J. Mater. Chem.* **2006**, *16*, 32.
[24] J. W. Choi, A. H. Flood, D. W. Steuerman, S. Nygaard, A. B. Braunschweig, N. N. P. Moonen, B. W. Laursen, Y. Luo, E. DeIonno, A. J. Peters, J. O. Jeppesen, K. Xe., J. F. Stoddart, J. R. Heath, *Chem. Eur. J.* **2006**, *12*, 261.
[25] P. R. Ashton, V. Balzani, O. Kocian, L. Prodi, N. Spencer, J. F. Stoddart, *J. Am. Chem. Soc.* **1998**, *120*, 11190.
[26] R. Ballardini, V. Balzani, M. T. Gandolfi, L. Prodi, M. Venturi, D. Philp, H. G. Ricketts, J. F. Stoddart, *Angew. Chem. Int. Ed. Engl.* **1993**, *32*, 1301.
[27] P. R. Ashton, R. Ballardini, V. Balzani, S. E. Boyd, A. Credi, M. T. Gandolfi, M. Gómez-López, S. Iqbal, D. Philp, J. A. Preece, L. Prodi, H. G. Ricketts, J. F. Stoddart, M. S. Tolley, M. Venturi, A. J. P. White, D. J. Williams, *Chem. Eur. J.* **1997**, *3*, 152.
[28] M. Grün, I. Laner, K. K. Unger, *Adv. Mater.* **1997**, *9*, 254.
[29] G. Van Tendeloo, O. I. Lebedev, O. Collart, P. Cool, E. F. Vansant, *J. Phys. Condens. Matter* **2003**, *15*, S3037.
[30] C. T. Kresge, M. E. Leonowicz, W. J. Roth, J. C. Vartuli, J. S. Beck, *Nature* **1992**, *359*, 710.
[31] Y. Lu, R. Ganguli, C. A. Drewien, M. T. Anderson, C. J. Brinker, W. Gong, Y. Guo, H. Soyez, B. S. Dunn, M. H. Huang, J. I. Zink, *Nature* **1997**, *389*, 364.
[32] M. H. Huang, B. S. Dunn, H. Soyez, J. I. Zink, *Langmuir* **1998**, *14*, 7331.
[33] J. M. Miller, B. S. Dunn, J. S. Valentine, J. I. Zink, *J. Non-Cryst. Solids* **1996**, *202*, 279.
[34] B. C. Dave, J. M. Miller, B. S. Dunn, J. S. Valentine, J. I. Zink, *J. Sol-Gel Sci. Technol.* **1997**, *8*, 629.
[35] B. S. Dunn, J. M. Miller, B. C. Dave, J. S. Valentine, J. I. Zink, *Acta Mater.* **1998**, *46*, 737.
[36] S. Chia, U. Jun, F. Tamanoi, B. S. Dunn, J. I. Zink, *J. Am. Chem. Soc.* **2000**, *122*, 6488.
[37] P. N. Minoofar, B. S. Dunn, J. I. Zink, *J. Am. Chem. Soc.* **2005**, *127*, 2656.
[38] C. J. Brinker, G. W. Scherer, in *Sol-Gel Science; The Physics and Chemistry of Sol-Gel Processing*, ACADEMIC PRESS, Boston, 1990, Chapter 3.
[39] A. Monnier, F. Schüth, Q. Huo, D. Kumar, D. Margolese, R. S. Maxwell, G. D. Stucky, M. Krishnamurty, P. Petroff, A. Firouzi, M. Janicke, B. F. Chmelka, *Science* **1993**, *261*, 1299.
[40] X. S. Zhao, G. Q. Lu, A. K. Whittaker, G. J. Millar, H. Y. Zhu, *J. Phys. Chem. B* **1997**, *101*, 6525.
[41] I. Haller, *J. Am. Chem. Soc.* **1978**, *100*, 8050.
[42] J. I. Zink, *Inorg. Chem.* **1975**, *14*, 555.
[43] V. Balzani, F. Barigelletti, L. De Cola, *Top. Curr. Chem.* **1990**, *158*, 31.
[44] A. C. Benniston, A. Harriman, V. M. Lynch, *J. Am. Chem. Soc.* **1995**, *117*, 5275.
[45] A. Ponce, H. B. Gray, J. R. Winkler, *J. Am. Chem. Soc.* **2000**, *122*, 8187.
[46] P. N. Minoofar, R. Hernandez, S. Chia, B. S. Dunn, J. I. Zink, A.-C. Franville, *J. Am. Chem. Soc.* **2002**, *124*, 14388.
[47] R. Hernandez, A.-C. Franville, P. Minoofar, B. S. Dunn, J. I. Zink, *J. Am. Chem. Soc.* **2001**, *123*, 1248.
[48] S. G. Entelis, O. V. Nesterov, *Russ. Chem. Rev.* **1996**, *35*, 917.
[49] M. H. Lim, A. Stein, *Chem. Mater.* **1999**, *11*, 3285.
[50] Y. Liu, A. H. Flood, J. F. Stoddart, *J. Am. Chem. Soc.* **2004**, *126*, 9150.
[51] A. C. Benniston, A. Harriman, D. Philp, J. F. Stoddart, *J. Am. Chem. Soc.* **1993**, *115*, 5298.
[52] M. Alvaro, B. Ferrer, V. Fornes, H. García, J. C. Scaiano, *J. Phys. Chem. B* **2002**, *106*, 6815.
[53] M. Alvaro, H. García, S. García, F. Márquez, J. C. Scaiano, *J. Phys. Chem. B* **1997**, *101*, 3043.
[54] J. C. Scaiano, H. García, *Acc. Chem. Res.* **1999**, *32*, 783.
[55] K. A. King, M. F. Finlayson, P. J. Spellane, R. J. Watts, *Sci. Pap. Inst. Phys. Chem. Res. Jpn.* **1984**, *78*, 97.
[56] Q. Jiang, A.-M. Spehar, M. Hakansson, J. Suomi, T. Ala-Kleme, S. Kulmala, *Electrochim. Acta* **2006**, *51*, 2706.
[57] P. R. Ashton, J. Huff, S. Menzer, I. W. Parsons, J. A. Preece, J. F. Stoddart, M. S. Tolley, A. J. P. White, D. J. Williams, *Chem. Eur. J.* **1996**, *2*, 31.
[58] A. R. Bernardo, J. F. Stoddart, A. E. Kaifer, *J. Am. Chem. Soc.* **1992**, *114*, 10624.
[59] J. E. Collins, J. S. Lamba, C. Love, J. E. McAlvin, C. Ng, B. P. Peters, X. Wu, C. L. Fraser, *Inorg. Chem.* **1999**, *38*, 2020.

© 2007 WILEY-VCH Verlag GmbH & Co. KGaA, Weinheim